287

CONCEPT STUDY OF A UV CORONAGRAPH SPECTROMETER

FOR THE

PINHOLE/OCCULTER FACILITY

Grant NAG 8-554

Final Report

For the period 1 October 1985 through 30 November 1985

Principal Investigator
Dr. John L. Kohl

July 1986

Prepared for
National Aeronautics and Space Administration
George C. Marshall Space Flight Center
Marshall Space Flight Center, AL 35812

by

Smithsonian Institution
Astrophysical Observatory
Cambridge, MA 02138

The Smithsonian Astrophysical Observatory
is a member of
Harvard-Smithsonian Center for Astrophysics

The NASA Technical Officer for this grant is Mr. Joseph R. Dabbs, George C. Marshall Space Flight Center, Marshall Space Flight Center, AL 35812

CONCEPT STUDY OF A UV CORONAGRAPH SPECTROMETER

FOR THE

PINHOLE/OCCULTER FACILITY

Grant NAG 8-554

Final Report

For the period 1 October 1985 through 30 November 1985

Principal Investigator
Dr. John L. Kohl

July 1986

Prepared for
National Aeronautics and Space Administration
George C. Marshall Space Flight Center
Marshall Space Flight Center, AL 35812

by

Smithsonian Institution
Astrophysical Observatory
Cambridge, MA 02138

The Smithsonian Astrophysical Observatory
is a member of
Harvard-Smithsonian Center for Astrophysics

The NASA Technical Officer for this grant is Mr. Joseph R. Dabbs, George C. Marshall Space Flight Center, Marshall Space Flight Center, AL 35812

TABLE OF CONTENTS

ABSTRACT

This report summarizes the results of a very short study to define an Ultraviolet Coronagraph-Spectrometer (UVCS) for the Pinhole/Occulter Facility (P/OF). The study is based on documentation from the Definition Phase of the Spacelab Coronagraphs Program which was effectively completed in August 1980. The primary differences between the P/OF instrument and the Spacelab experiment are the remote occulter mask, the telescope size and the deployable structure to accommodate P/OF's length restrictions. Requirements for P/OF that are associated with these features are briefly considered in this report, but further study is needed to more fully consider their unusual implications—particularly in the interplay between the instrument pointing and the P/OF boom control.

1. INTRODUCTION

Improved knowledge of the physical condition throughout the solar corona is critical to the development of an understanding of the physical state of the corona and the physical processes responsible for plasma heating, solar wind acceleration, energetic particle acceleration and the transport of mass, momentum, and energy. Ultraviolet spectroscopic data acquired by the UVCS on P/OF can greatly expand empirical information about temperatures, densities, flow velocities and chemical abundances in the corona to $r \geq 10\ R_{\odot}$. Such information would provide tight empirical constraints on critical processes involved in the transport and dissipation of energy and momentum, the heating and acceleration of plasma and the acceleration of energetic particles. Because of its high sensitivity, high spatial and temporal resolutions, and powerful capabilities for plasma diagnostics, the P/OF-UVCS can significantly increase our knowledge of coronal streamers and transients, and thereby

advance the understanding of the physics of these phenomena. The P/OF-UVCS can provide the first observations capable of establishing the role in solar wind generation of small-scale dynamical phenomena, such as spicules, macrospicules and coronal "bullets", and the role of the fine-scale structures, such as polar plumes. Since the P/OF mask also serves as a multi-pinhole array for high resolution hard x-ray imaging, simultaneous measurements by the UVCS and hard x-ray instruments can provide critical empirical information concerning non-thermal energy releases and acceleration of energetic particles in the corona.

Because the P/OF occulting mask is large and is located much farther (~50 m) from the telescope mirror than for any previous externally occulted coronagraphic instrument, it is possible to employ telescopes of large aperture (~0.5 m). This gives the P/OF-UVCS sufficient collecting area to have about a factor of 100 higher sensitivity than any normally sized UVCS. As a result, the P/OF-UVCS can provide measurements with high spatial resolution (~1 arc second—more than 2 orders of magnitude better than previous UV observations of the extended corona), and it can provide good time resolution for UV studies of transient phenomena, as well as provide a capability for measuring weak coronal lines at large distances from the sun.

In summary, the P/OF-UVCS is a unique and powerful tool that offers unprecedented capabilities for studying the source region of the solar wind, coronal transients and the acceleration of energetic particles. The data are expected to be used to identify the coronal structures and physical processes responsible for energy and momentum transport and for energy and momentum deposition. Identification of these mechanisms in the sun will help make possible development of realistic physical models for stellar wind acceleration in late type stars.

The P/OF-UVCS is a direct evolutionary step from the conventionally sized Ultraviolet Coronal Spectrometer that has been used successfully on three sounding rocket flights and is now being readied for Spartan Missions. The P/OF-UVCS described in this report, is based (in part) on the results of a definition study for a Spacelab Lyman Alpha Coronagraph (SLAC). For P/OF, the spectrograph design including most of the mechanisms and much of the electronics is retained. The emphasis for the present study is on the large telescope, the support structure and deployment mechanism and on the accommodation and alignment of the instrument at the P/OF instrument plane.

Both the Spacelab Definition Phase and the present study were carried out together with Ball Aerospace Systems Division, Boulder, Colorado.

2. INSTRUMENT LAYOUT

To achieve the scientific objectives discussed above, the specifications provided in Table 1 are required. The instrument layout for the P/OF-UVCS is illustrated in Figure 1 and its accommodation behind the P/OF mask is shown in Figure 2. The spectrometer is illustrated in Figure 3.

The P/OF-UVCS consists of a 44 cm x 44 cm telescope of 3.5 m focal length (see Table 2) and a 1.5 m spectrometer with two-dimensional array detectors. The telescope is shielded from direct sunlight by the P/OF mask which acts as a linear straight edge occulter. The entrance aperture to the instrument case (located 5.5 m from the telescope mirror) shields the telescope from stray light off the boom and the nearby space hardware. A moveable internal occulter is located near the telescope mirror. The internal occulter is located just in front of the mirror surface, and its position across the mirror surface is set to intercept diffracted light from the P/OF mask edge

that would otherwise be directed into the spectrometer by the telescope mirror. Internal baffles are used to further reduce scattered light. Direct sunlight also enters the UVCS entrance aperture where it is intercepted by two mirrors and discarded. The spectrometer specifications are provided in Table 3. This spectrometer has characteristics that are generally satisfactory, but the design has not yet been optimized for the P/OF application.

3. OPTICAL PERFORMANCE

This study assumes the use of the SLAC spectrometer design with minor modifications. Detectors are to be 1024 x 1024 pixel multianode coincident arrays rather than the original discrete anode arrays. The pixel separation is 25.4 μm. If a 25.4 μm entrance slit is used, the instantaneous field of view (IFOV) in the cross-slit (solar radial) direction is 1.5 arc second. A 17 μm slit will restrict the IFOV to 1 arc second in the solar radial direction. Along the slit, spatial resolution is 3 arc second, considering a pixel pair to be one resolution element. There is potential for subpixel resolution, spatial and spectral, by dithering some element of the system. The spectral resolution is detector limited at .094 Å/pixel.

A computer ray-trace model of the P/OF-UVCS was set up for this study using the ACCOS V program. Imaging was evaluated at the entrance slit of the spectrometer as a function of field angle. The telescope mirror is used on axis when viewing 4.25 $R_\odot$ and is tilted to view other points along a solar radius. A slit length of 25.4 mm (equal to 25 arc minutes FOV) is assumed so as to use the full area of the detector. Geometrical spot diagrams were generated for various field angles, and the results are summarized in Table 4.

At the center of the field, 4.25 $R_\odot$, the image is diffraction limited at 1 μm FWHM or .06 arc seconds at 1216 Å. At the slit ends, still at 4.25 $R_\odot$, aberrations spread the image to 34.2 μm RMS. At slit center, scanning from 1.1 $R_\odot$ to 7.4 $R_\odot$, the geometrical image is at first small (17 μm due to extreme vignetting of the mirror), increases to 36 μm at 2.25 $R_\odot$, goes to minimum at 4.25 $R_\odot$ on axis and then grows to 70 μm at the 7.4 $R_\odot$ extreme.

4. THE OCCULTERS

Vignetting by the P/OF occulter decreases linearly from total at 1.1 $R_\odot$ to zero at 3.0 $R_\odot$. An internal occulter similar to the one used on SLAC must be provided to obstruct light scattered by the P/OF occulter edge. For SLAC, the internal occulter was driven across the mirror by the same mechanism that scanned the mirror, thereby coordinating the occulter with the direction of viewing. On P/OF, the exact location of the occulter shadow may not be predictable; therefore, there is a need to independently position the internal occulter.

The internal occulter will move linearly with angle of view:

$$S = A\theta + B$$

S = occulter edge location

θ = angle of view

A is the distance to the P/OF occulter, assumed to be 50 meters, and is fixed. B is a zero offset and depends on the coalignment of UVCS to P/OF. This means that a single mechanism could still coordinate both motions, but an offset capability would be added which could be experimentally adjusted while viewing close to the limb.

Alternatively, two separate drives could be coordinated through a microprocessor so that the internal occulter position could be any specified function of the mirror angle; this would be a more flexible and more expensive approach.

5. SUNLIGHT REJECTION

Two mirrors arranged as shown in Figure 4 can reject the light from the solar disk that unavoidably enters the UVCS aperture. By rejecting the light to the side away from the other experiments, there should be no interference with them and no backscatter from particles in the field of view. Also, the heat buildup that would occur in a trap is avoided. The mirrors are positioned so that neither are within the acceptance angle of the spectrometer entrance slit.

6. SOLAR POINTING AND OCCULTER ALIGNMENT

In the Visidyne study, "Pinhole X-Ray Coronagraph Optical Systems Concept Definition," a pointing system is described with independent solar and occulter direction sensors located on the instrument platform. When the occulter is deployed on orbit, there will be an error ωr in the location of the occulter which results in a displacement of ωr of the shadow of the occulter. This will be corrected by biasing the pointing of the P/OF through an angle of $-\omega r/50$ to realign the shadow with the instruments. A mask alignment mechanism provides roll about the mask axis to align the occulter with the instruments in roll. The $-\omega r/50$ pointing compensation will leave the UVCS misaligned relative to the sun by the angle $-\omega r/50$. Also, the front aperture of the instrument will be misaligned by $-5.5\ \omega r/50$.

One effect of the misalignment will be to change the direction of best, on axis, imaging. About ~0.5 $R_\odot$ of this is tolerable without substantial image degradation. This corresponds to ωr = ~12 cm. The corresponding displacement of the UVCS aperture is 1.3 cm. This would cause up to 3% vignetting at some view angles, and the heat dump mirrors would have to be oversized to accommodate this.

It is recommended that, if ωr is anticipated to be greater than ~10 cm, a coalignment capability be incorporated in the UVCS mounting so that the whole instrument can tilt to compensate for realignments of the P/OF platform due to displacements of the P/OF occulter. When the design and performance of P/OF is determined, this aspect of the UVCS should undergo further study.

7. INSTALLATION ON P/OF

When stowed in the STS cargo bay, the P/OF and its associated Instrument Pointing System (IPS) will occupy two pallets. This limits the length of instruments mounted on the platform to 3 meters; so it is necessary to deploy the UVCS from a 3 meter configuration to a little more than 5.5 meters. The method by which this is done must also:

(1) Withstand launch environment;

(2) Protect against contamination in both configurations;

(3) Reject stray light when deployed;

(4) Regain optical alignment when deployed;

(5) Fit in the allowed envelope; and

(6) Deploy and stow reliably.

A hinged concept based on a configuration already proposed is shown in Figure 5. A cover plate is added to protect both halves when stowed and folds

against the lower half when deployed. In this view (plane of dispersion), the deployed instrument is 1.4 meters wide to accommodate and protect the spectrometer, the telescope mirror, and the heat rejection mirrors. When stowed, the package is 3 meters wide, which is too large. One solution to this is to hinge the instrument so that it swings out of the plane of the drawing. The instrument case is about 0.5 meters deep; so, this way the stowed package would be 2 x 1.4 x 1.1 meters. Also, by swinging in this plane, it would never be in the Fourier transform X-ray instrument's space. The hinging should use two precision bearings, and there should be one hard stop to kinematically locate the front end of the instrument so that the location of the spectrometer slit repeats to ~0.15 mm when deployed. Deployment should be done with the P/OF pointed opposite to the velocity of the spacecraft to avoid sweeping up contaminants with the instrument. This configuration is shown on the platform in Figure 2. As shown, the package is crammed up against the boom. More detailed study and design will reveal how close this actually is. Since the spectrometer is narrower than the mirror, the whole package could be narrowed down near the boom if necessary. The boom would also interfere with the opening the protective cover as drawn in Figure 5; so, it will need to swing in another direction.

A telescoping mechanism is attractive because the stowed volume is smaller, and it does not swing through large arcs. Such a concept is shown in Figures 1 and 6. The forward section comprising the spectrometer and front aperture is smaller in cross section than the aft section housing the mirror and deployment drive and can fit within it. Three long drive screws with recirculating ball nuts move the forward section from its stowed location within the aft section to its fully forward deployed position. The screws are synchronously driven by roller chain and sprockets. At the extremes of

travel, flanges seal and protect the interior of the instrument from stray light and contamination. This is the only one one of the three deployment schemes that easily fits in the available area on the mounting platform, and it has no need for extra cover mechanisms. If further study and design demonstrates the practicality of the concept, it is clearly the preferable choice.

8. MASS PROPERTIES

A very rough estimate was made of the weight, center of gravity (CG), and moments of the P/OF-UVCS. The weight and CG of the spectrometer was taken from earlier SLAC studies and should be quiet accurate. The estimates for the new case and deployable configuration are based on the assumption of a ribbed aluminum structure of 0.1 inches average thickness. The mass properties are listed in Tables 5 and 6 for stowed and deployed configurations, and the coordinate axes are indicated in Figure 1.

9. ELECTRONICS

The UVCS electronics will be the same as SLAC, except for the detector electronics and the addition of a motor and drive electronics for deploying and stowing the instrument. The SLAC detectors were discrete-anode microchannel arrays with 241 discrete anodes. On P/OF-UVCS, we will use two 1024 x 1024 coincidence array MAMAs. These increase the data rate by a factor of 20, from 5 x 104 bit/sec for SLAC to 1 Megabit/second for P/OF-UVCS which is accommodated by the CDMS's high rate multiplexer. The power consumption increase due to the addition of the deployment mechanism is nominal, about 20 watts for 1 minute for each actuation. The larger instrument, however, will require more heater power; how much depends on the not yet known thermal

interface with the P/OF and the IPS, and whether a thermal shroud or canister encloses the instrument cluster.

The electronics are located both remotely with each MAMA detector and in a central electronics support box. The remote electronics include high voltage power supplies and signal conditioning circuits; its output is a digital pixel address code. The central electronics includes digital signal processing, a microprocessor for control and sequencing, motor drive circuits, power conditioning and power distribution, and interfacing circuits to the IPS experiment remote acquisition unit (RAU). The MAMA detector circuits are implemented with hybrid circuitry to minimize size, while the central electronics use conventional discrete components. The MAMA signal levels are fairly high (5×10^6 electrons) due to the MCP amplification. These are easily detected by conventional FET amplifiers that can be built in both discrete and hybrid forms. Components such as the microprocessor are generally low power and radiation hardened for long life. Self test circuits allow for rapid verification.

A block diagram of the overall SLAC electronics is shown in Figure 7. The shaded area in the SLAC block diagram gets replaced by the diagram in Figure 8 to become the P/OF-UVCS electronics block diagram. The MAMA detectors each have row and column pulse event detectors on every channel. These consist of a charge pre-amplifier, followed by shaping, lower level discriminator (LLD) and sample/hold circuits. The row and column pulses are monitored by a pixel address encoder which outputs a pixel address code to the central digital processor. There an event header that is formatted with a time tag and sent to the ground via the CDMS. Non-UV events are determined by simultaneous signals in a row or column, and these are discarded at the encoder. The instrument microprocessor accepts commands from the the CDMS to

initiate control sequences for the motor drives and to apply HV to the MAMA detectors. A vacion pump is attached to each MAMA for use in ground testing.

TABLE 1

P/OF-UVCS REQUIREMENTS

SPATIAL RESOLUTION:	1 ARC SECOND GOAL
SPECTRAL RESOLUTION:	.08 Å GOAL
FIELD OF REGARD:	1.1 TO 7.4 $R_\odot$
SPEED:	F/8
FOCAL LENGTH:	3.5 M
LENGTH (STOWED):	3.0 M MAX
SPECTROMETER:	AS IN SLAC (SEE TABLE 3)
DETECTORS:	TWO 1024 × 1024 MAMAs

TABLE 2

OPTICAL CHARACTERISTICS OF P/OF-UVCS TELESCOPE

TYPE	SCANNING OFF-AXIS PARABOLOID
FOCAL LENGTH	3.50 ≥.03 M
MIRROR SIZE-CLEAR APERTURE	44 X 44 CM
OFF-AXIS DISTANCE, MIRROR CENTER TO IMAGE POINT	33.5 CM
SPEED	F/8
FRONT APERTURE	51.6 X 48 CM, 550 CM FROM MIRROR
TOTAL FIELD OF VIEW	25 X 100 ARC MINUTE
INSTANTANEOUS FIELD OF VIEW (IFOV)	25 X (.025,TBD) ARC MINUTE DEPENDING ON ENTRANCE SLITS
IMAGE SCALE	1.02 MM/ARC MINUTE
IMAGE QUALITY	DIFFRACTION LIMITED FOR VISIBLE LIGHT
COATING	BIPARTITE, Al/MgF_2 & IRRIDIUM
SURFACE FINISH	20/10 SCRATCH/DIG
SCAN PIVOT LOCATION	CENTER OF MIRROR FACE
RANGE (MINIMUM)	100 ARC MINUTE
INCREMENT (MAXIMUM)	1.0 ARC SECOND REFERRED TO
READOUT PRECISION (MAXIMUM)	1.0 ARC SECOND IMAGE MOTION
REPEATABILITY (RMS)	1.0 ARC SECOND
VIGNETTING	COMPLETE AT 1.1 R_o
	ZERO AT 3.0 R_o FIELD ANGLE

TABLE 3
P/OF-UVCS SPECTROMETER CHARACTERISTICS

TYPE	SCANNING ROWLAND-CIRCLE SPECTROMETER
GRATING TYPE	CONCAVE TOROIDAL REPLICA OF MECHANICALLY-RULED MASTER
RULING FREQUENCY	1800 GROOVES/MM
RADIUS-DISPERSION	1500 ≥ 5 MM RATIO - 1.0273 ≥ 0.0005
RADIUS-CROSS	1460 ≥ 5 MM
SIZE-CLEAR APERTURE	257 MM (DISPERSION) X 225 MM (GROOVE LENGTH) 257 MM DIMENSION INCLUDE 25 MM OF 400.7 G/MM RULING FOR VISIBLE SPECTRUM ALIGNMENT
BLAZE	1032 A, FIRST ORDER
COATING	BIPARTITE, Al/MgF_2 + IRRIDIUM
ENTRANCE SLITS	17 µM X 25.4 MM LONG 25 µM X 25.4 MM LONG TBD µM X 25.4 MM LONG TBD µM X 25.4 MM LONG
ANGLE OF INCIDENCE	13.2486⟩
ANGLE OF DIFFRACTION	-0.58996⟩ AT 1216 A -0.32180⟩ AT 1242 A AT CENTRAL -2.56062⟩ AT 1025 A GRATING +3.78650⟩ AT 1640 A POSITION -4.67878⟩ AT 820 A
SPATIAL RESOLUTION (WITH TELESCOPE)	1.5 ARC SECOND (RADIAL) 3.0 ARC SECOND (TANGENTIAL)
RECIPROCAL DISPERSION	3.7085 A/MM WITH FIXED GRATING
SPECTRAL RESOLUTION	0.094 A WITH 25 µM SLIT
SPECTRAL STRAY LIGHT	TBD
SCAN SCALE FACTOR	95.75 A/DEGREE
PIVOT LOCATION	CENTER OF ROWLAND CIRCLE
MINIMUM RANGE	+3.25 (CCW) TO -4.43 (CW)
INCREMENT	0.005 A
READOUT PRECISION	0.005 A
REPEATABILITY	0.005 A
SPEED	FULL RANGE IN 60 SECONDS MAXIMUM

TABLE 4

GEOMETRICAL RAY TRACE RESULTS AT P/OF-UVCS TELESCOPE FOCAL PLANE

Field Point [1]						
Radial (R_o)	Tangential (R_o)	Astigmatism[2] (mm)	% Through 25.4 μm slit [3]	% Within 25.4 μm square	Geometric RMS Radius (μm)	Spatial Resolution [4] (sec.)
4.25	0	0	100	100	0	1.5
3.25	0	.76	74	50	21.5	1.5
2.25	0	1.9	37	15	36.5	2.1
1.25	0	3.3	70	38	17.6	1.5
7.25	0	2.5	45	9.5	69.7	4.1
7.25	0.78	2.5	35	1.7	78.6	4.6
4.25	0.78	0.05	38	12	34.2	2.0

1. Field point is in units of solar radii (R_o).
2. Astigmatism is the distance between the best tangential and sagital foci.
3. Percent of light reaching the slit plate that is passed, vignetting not included.
4. Spatial resolution = RMS radius x .059 arc sec/μm. 1.5 arc sec. minimum is the diffraction limit.

Table 5 P/OF-UVCS mass properites for telescoping deployment concept (stowed configuration)

UVCS RAW MASS PROPERTIES DATA , NO CONTINGENCY ADDED NOTE, ALL MOMENTS ARE ABOUT C. G. 85-10-10 H. V. ROYER

DESIGN MATURITY , E=ESTIMATED ,

		WEIGHT	C. G. COORDINATE			MOMENTS OF INERTIA			PRODUCTS OF INERTIA		
		(POUNDS)	(INCHES)			(LBS-INCHES SQUARED)			(LBS-INCHES SQUARED)		
CODE	ITEM DWG	WT	X	Y	Z	IXX	IYY	IZZ	PXY	PYZ	PXZ
SPECTROGRAPH											
10. 10. 01E	STRUCTURE, CASE	60. 000	27. 500	0. 000	79. 000	16. 943	20. 891	4. 547			
80. 10. 02E	GRATING & DRIVE	25. 000	24. 000	0. 000	104. 000	0. 000	0. 000	0. 000			
20. 10. 03E	DETECTORS	15. 000	20. 300	0. 000	42. 000	0. 000	0. 000	0. 000			
60. 10. 04E	ENTRANCE SLIT, ETC	5. 000	18. 750	0. 000	40. 000	0. 000	0. 000	0. 000			
10. 10. 05E	ATTACH BRKTS & HARDW	10. 000	27. 500	0. 000	79. 000	0. 000	0. 000	0. 000			
SUM		115. 000	25. 420	0. 000	77. 913	26. 362	30. 519	4. 757	0. 000	0. 000	0. 703
MAIN CASE (MOVEABLE)											
10. 20. 01E	CASE STRUCTURE	225. 000	14. 250	0. 000	58. 300	72. 828	86. 722	23. 354			
10. 20. 02E	FRONT DOOR ASSY	15. 000	0. 000	0. 000	118. 000	0. 000	0. 000	0. 000			
50. 20. 03E	THERMAL	8. 000	14. 250	0. 000	58. 300	0. 000	0. 000	0. 000			
SUM		248. 000	13. 388	0. 000	61. 911	83. 672	98. 184	23. 972	0. 000	0. 000	-2. 588
SUBTOTAL		363. 000	17. 200	0. 000	66. 980	114. 377	135. 502	31. 184	0. 000	0. 000	1. 380
MAIN CASE (FIXED)											
10. 30. 01E	CASE STRUCTURE	255. 000	14. 250	0. 000	60. 000	82. 538	98. 285	26. 468			
30. 30. 02E	PRIMARY MIRROR ASSY	50. 000	0. 000	0. 000	25. 000	0. 000	0. 000	0. 000			
80. 30. 03E	BALL SCREW ASSY (3)	180. 000	14. 250	0. 000	55. 000	0. 005	0. 007	0. 001			
30. 30. 04E	TRAP MIRRORS ETC	20. 000	0. 000	0. 000	15. 000	0. 000	0. 000	0. 000			
40. 30. 05E	ELECT BOXES	35. 000	25. 600	0. 000	15. 000	0. 000	0. 000	0. 000			
SUM		540. 000	13. 138	0. 000	50. 509	110. 282	129. 929	30. 367	0. 000	0. 000	3. 063
TOTAL		903. 000	14. 771	0. 000	57. 131	237. 374	278. 918	62. 324	0. 000	0. 000	7. 578

Table 6 P/OF-UVCS mass properties for telescoping deployment concept (deployed configuration)

UVCS RAW MASS PROPERTIES DATA , NO CONTINGENCY ADDED NOTE, ALL MOMENTS ARE ABOUT C. G. 85-10-10 H. V. ROYER

DESIGN MATURITY , E=ESTIMATED ,

		WEIGHT	C. G. COORDINATE			MOMENTS OF INERTIA			PRODUCTS OF INERTIA		
		(POUNDS)	(INCHES)			(LBS-INCHES SQUARED)			(LBS-INCHES SQUARED)		
CODE	ITEM DWG	WT	X	Y	Z	IXX	IYY	IZZ	PXY	PYZ	PXZ
SPECTROGRAPH											
10. 10. 01E	STRUCTURE, CASE	60. 000	27. 500	0. 000	195. 000	16. 943	20. 891	4. 547			
80. 10. 02E	GRATING & DRIVE	25. 000	24. 000	0. 000	220. 000	0. 000	0. 000	0. 000			
20. 10. 03E	DETECTORS	15. 000	20. 300	0. 000	158. 000	0. 000	0. 000	0. 000			
60. 10. 04E	ENTRANCE SLIT, ETC	5. 000	18. 750	0. 000	157. 000	0. 000	0. 000	0. 000			
10. 10. 05E	ATTACH BRKTS & HARDW	10. 000	27. 500	0. 000	195. 000	0. 000	0. 000	0. 000			
SUM		115. 000	25. 420	0. 000	193. 957	26. 281	30. 439	4. 757	0. 000	0. 000	0. 695
MAIN CASE (MOVEABLE)											
10. 20. 01E	CASE STRUCTURE	225. 000	14. 250	0. 000	174. 300	72. 828	86. 722	23. 354			
10. 20. 02E	FRONT DOOR ASSY	15. 000	0. 000	0. 000	234. 000	0. 000	0. 000	0. 000			
50. 20. 03E	THERMAL	8. 000	14. 250	0. 000	174. 000	0. 000	0. 000	0. 000			
SUM		248. 000	13. 388	0. 000	177. 901	83. 675	98. 188	23. 972	0. 000	0. 000	-2. 589
SUBTOTAL		363. 000	17. 200	0. 000	182. 988	114. 329	135. 454	31. 184	0. 000	0. 000	1. 383
MAIN CASE (FIXED)											
10. 30. 01E	CASE STRUCTURE	255. 000	14. 250	0. 000	60. 000	82. 538	98. 285	26. 468			
30. 30. 02E	PRIMARY MIRROR ASSY	50. 000	0. 000	0. 000	25. 000	0. 000	0. 000	0. 000			
80. 30. 03E	BALL SCREW ASSY (3)	180. 000	14. 250	0. 000	55. 000	0. 005	0. 007	0. 001			
30. 30. 04E	TRAP MIRRORS ETC	20. 000	0. 000	0. 000	15. 000	0. 000	0. 000	0. 000			
40. 30. 05E	ELECT BOXES	35. 000	25. 600	0. 000	15. 000	0. 000	0. 000	0. 000			
SUM		540. 000	13. 138	0. 000	50. 509	110. 282	129. 929	30. 367	0. 000	0. 000	3. 063
TOTAL		903. 000	14. 771	0. 000	103. 765	1047. 108	1088. 652	62. 324	0. 000	0. 000	29. 661

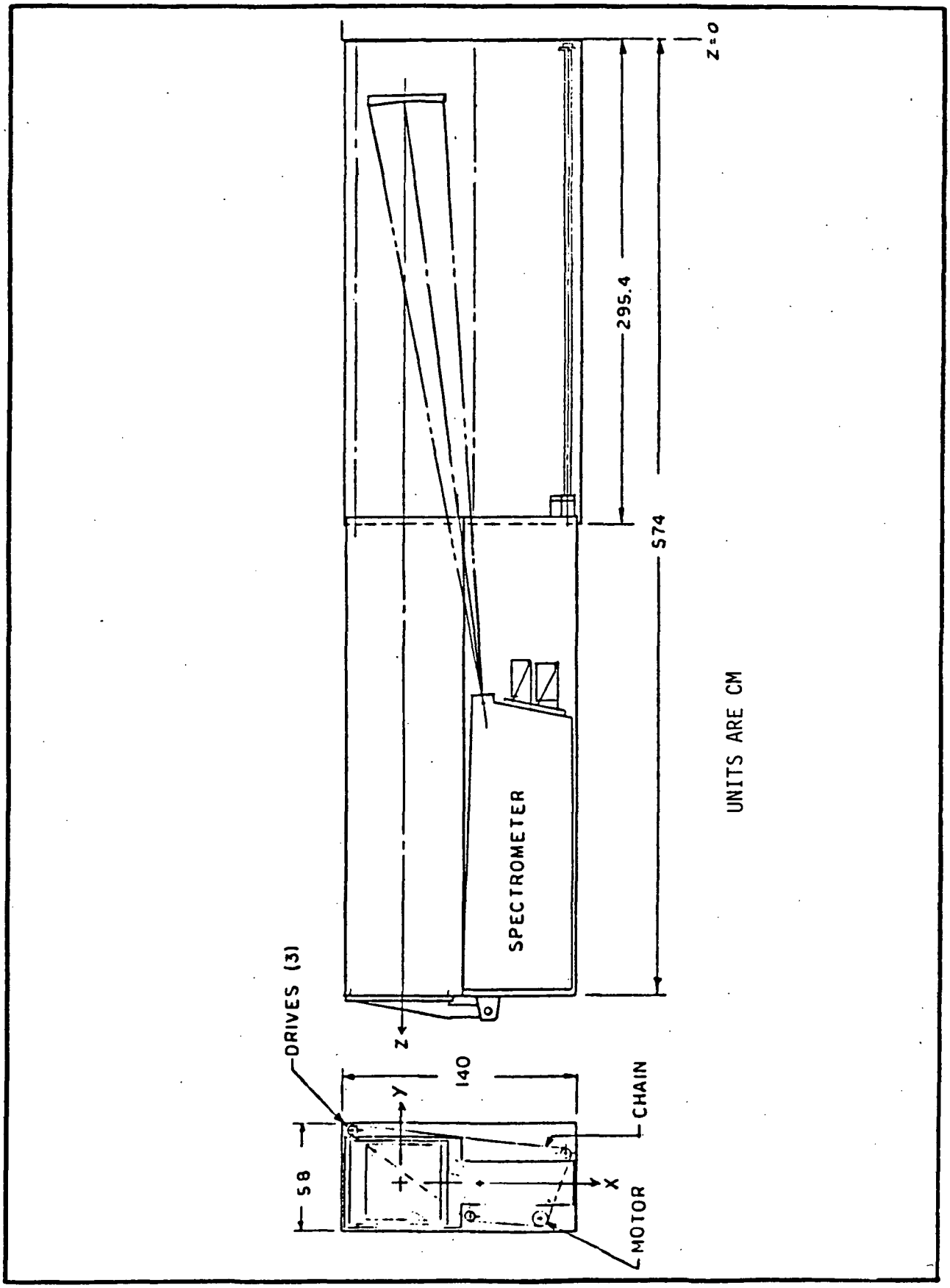

Figure 1. P/OF-UVCS Instrument Layout (showing telescoping deployment concept).

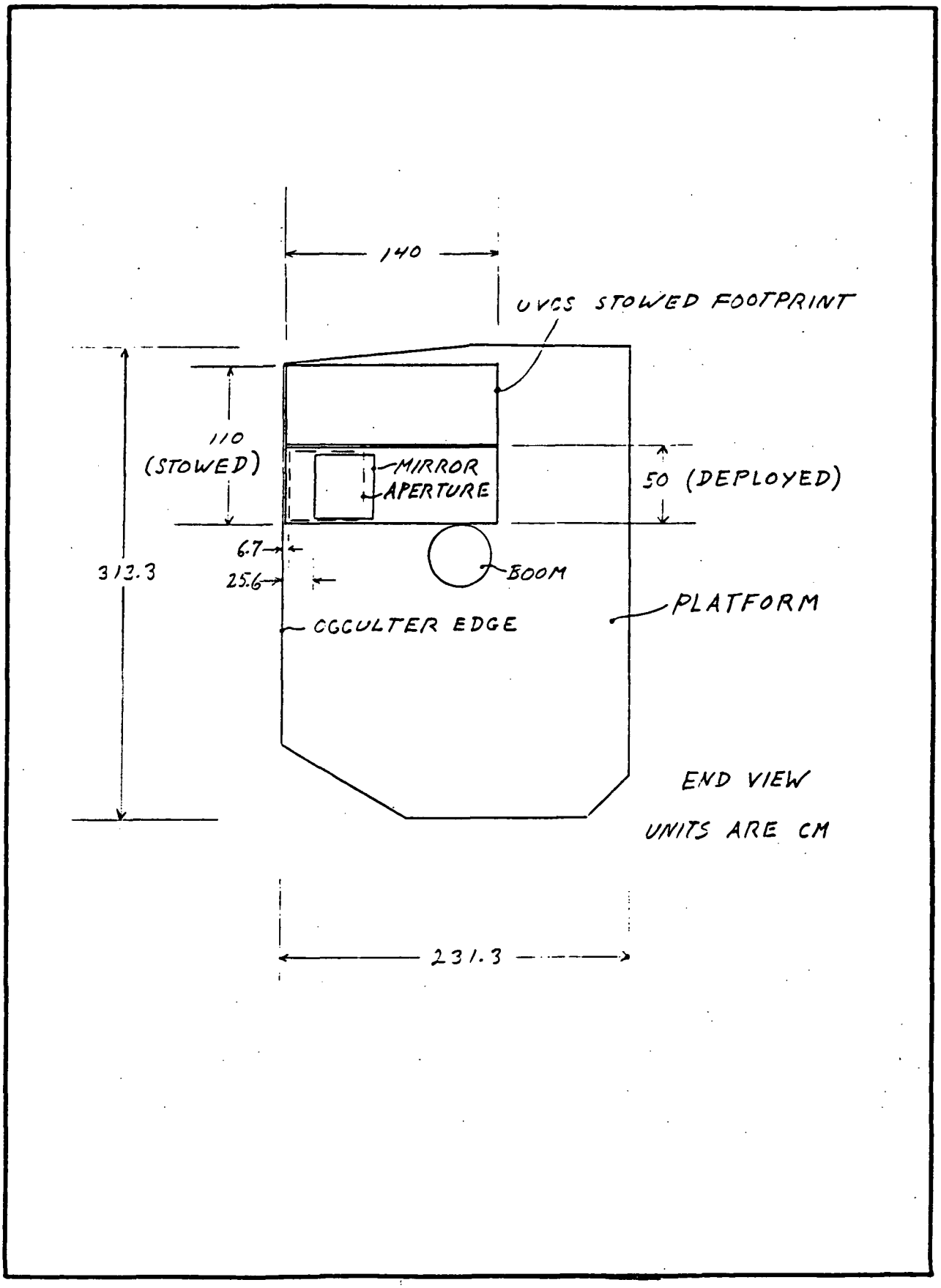

Figure 2. UVCS Alignment with P/OF Mask and Boom.

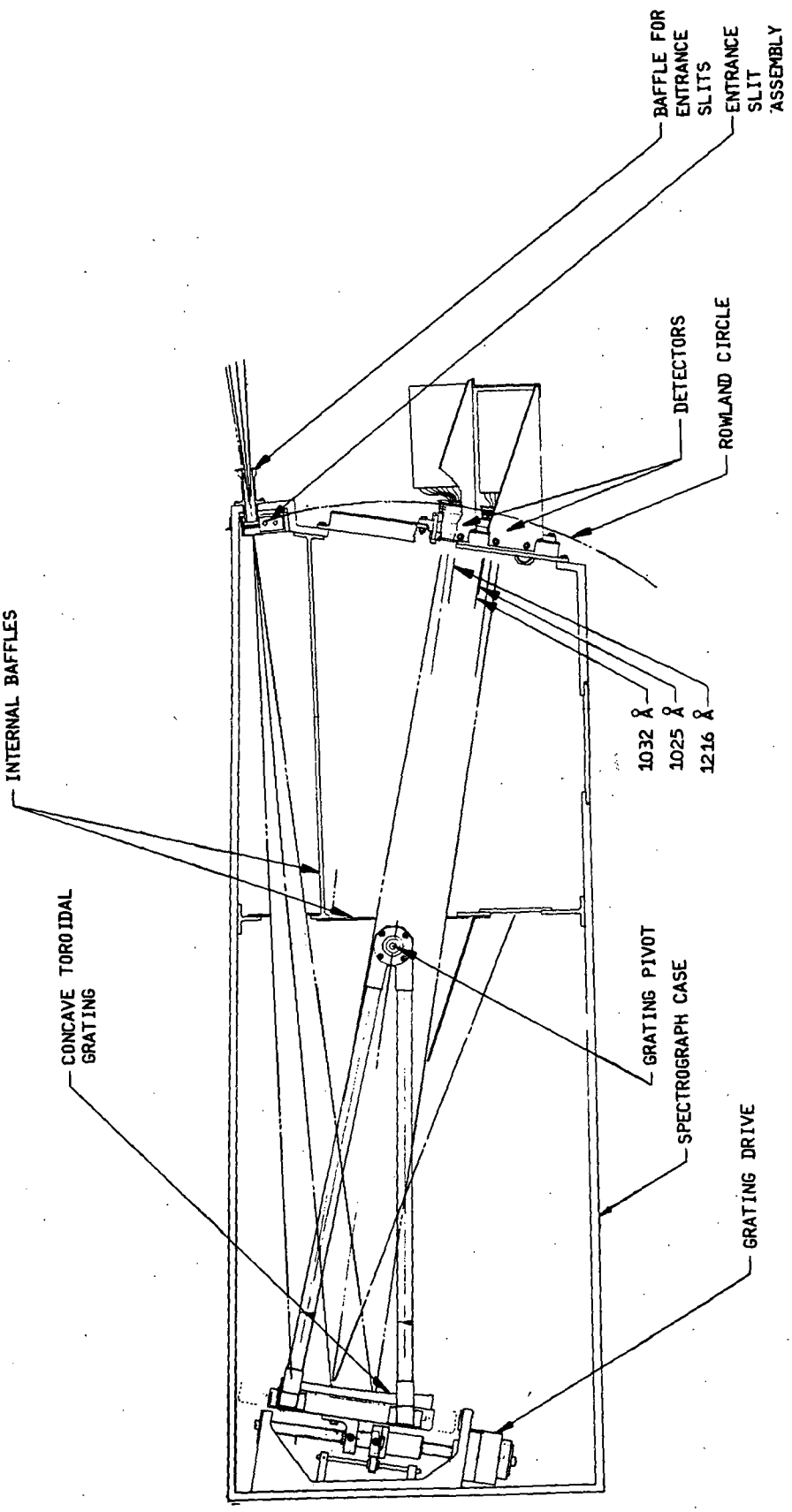

Figure 3. P/OF-UVCS Spectrometer Layout.

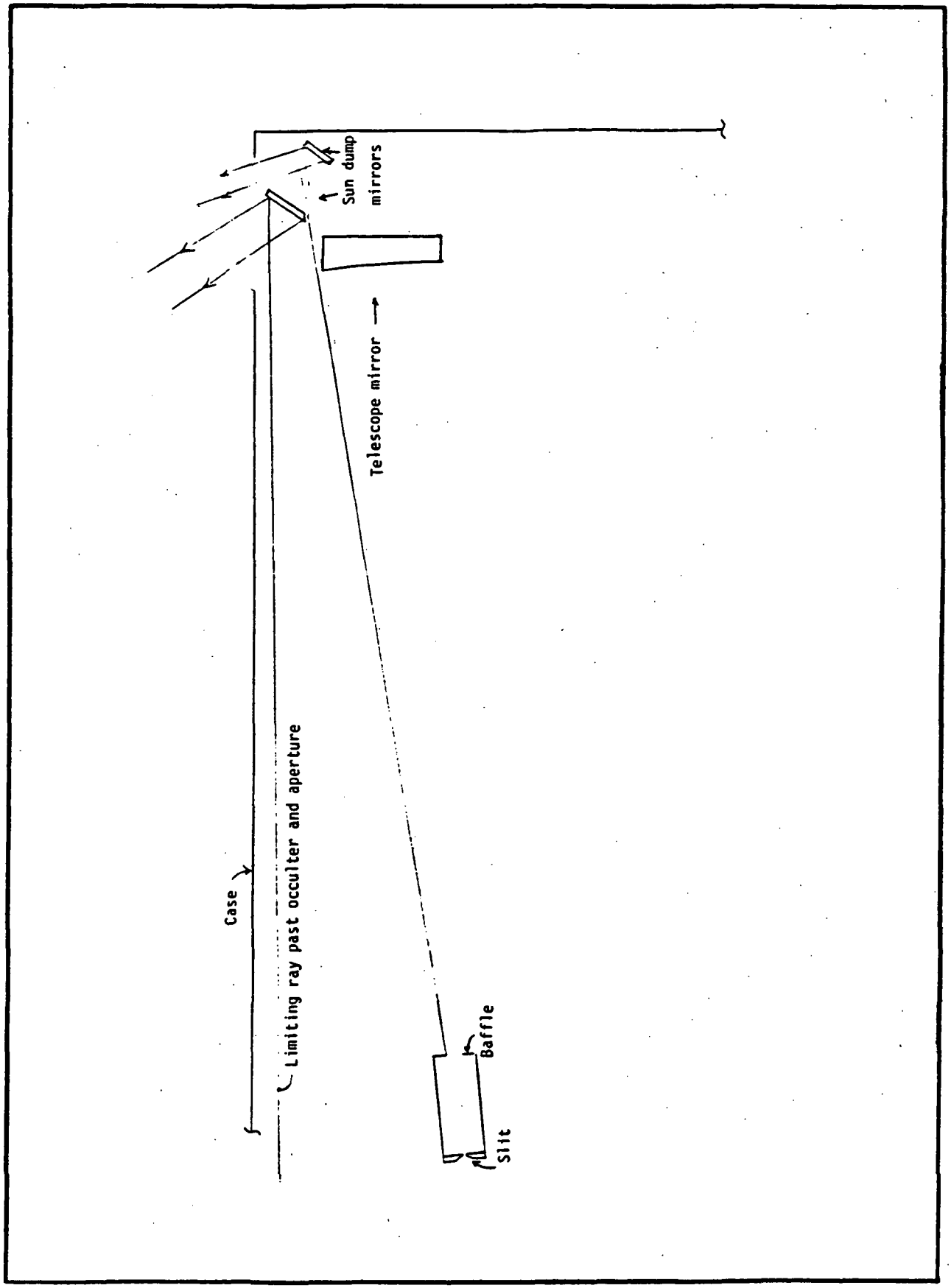

Figure 4. System for dumping sunlight without scatter to the spectrometer slit.

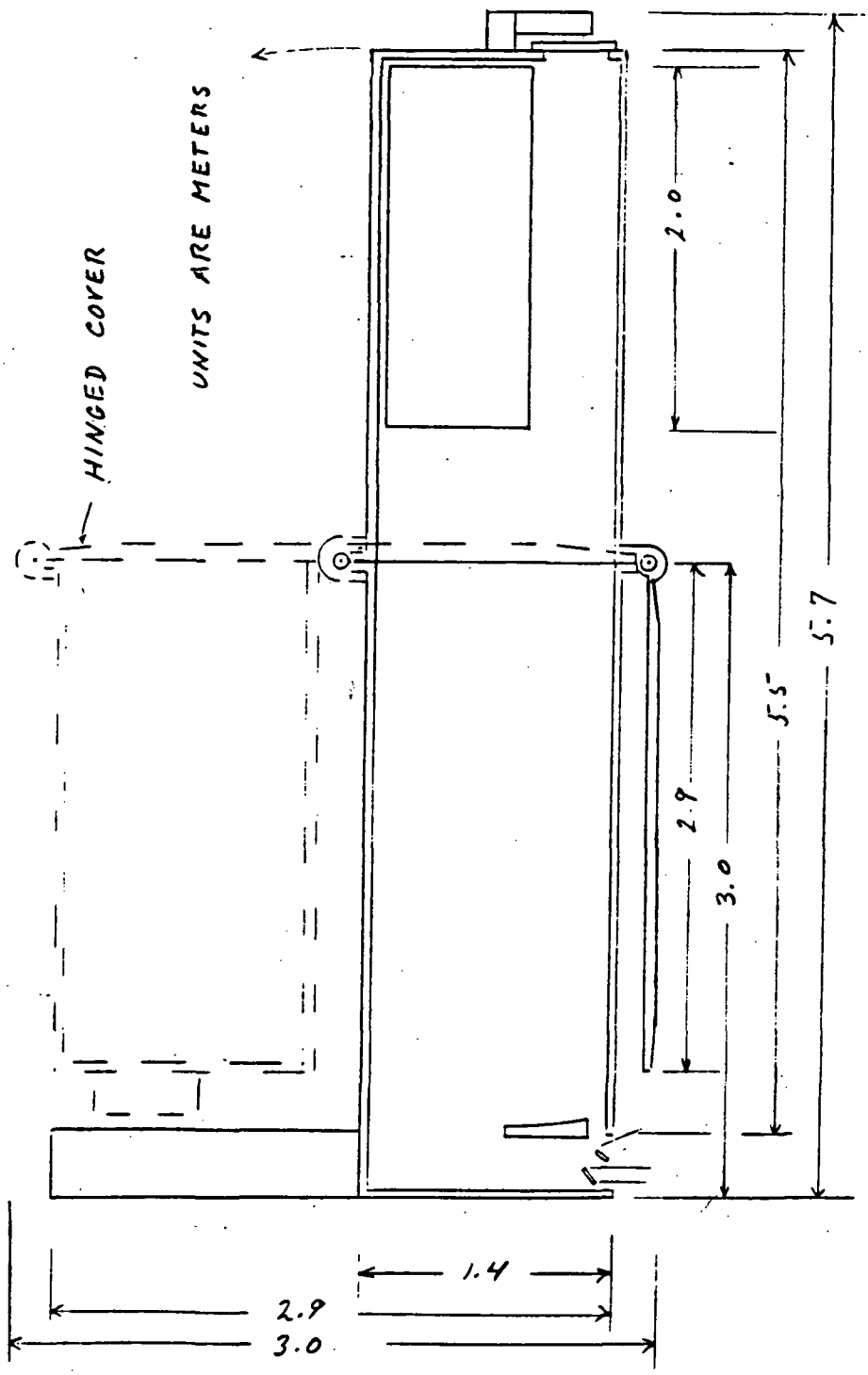

Figure 5. P/OF-UVCS Hinged Deployment Concept (the total width is too great for the P/OF platform).

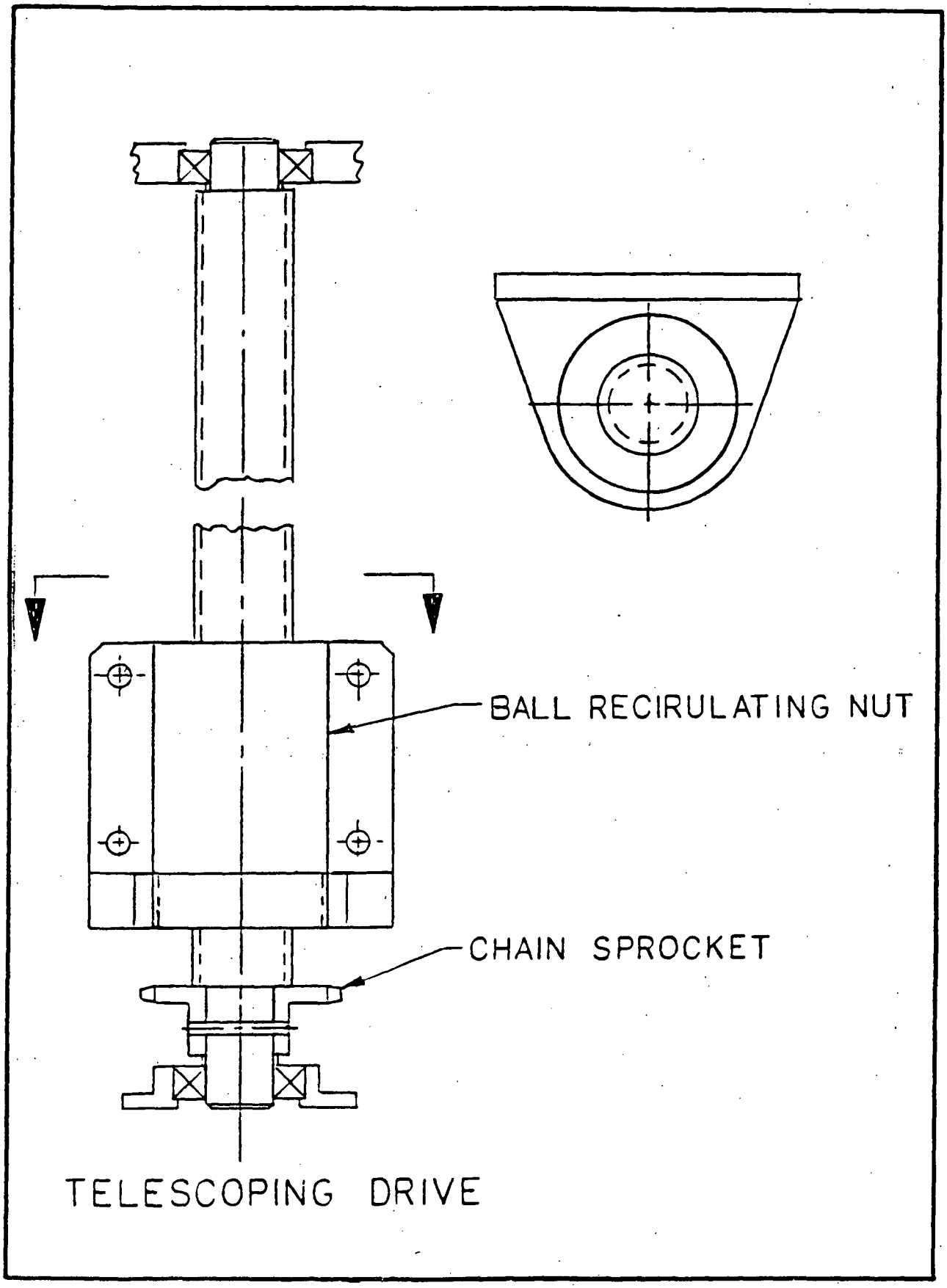

Figure 6. Drive for telescoping deployment concept.

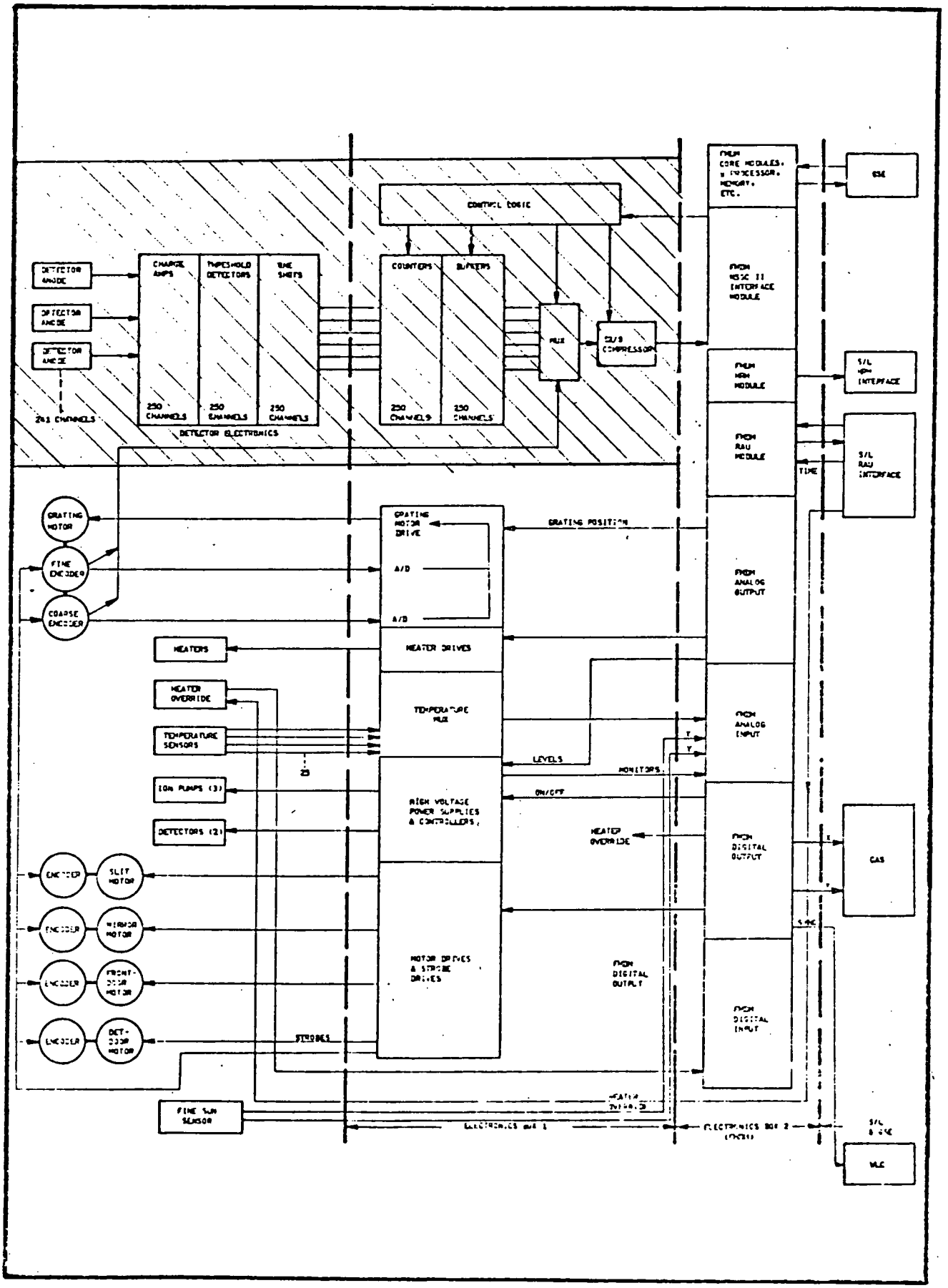

Figure 7. SLAC Electronics Block Diagram

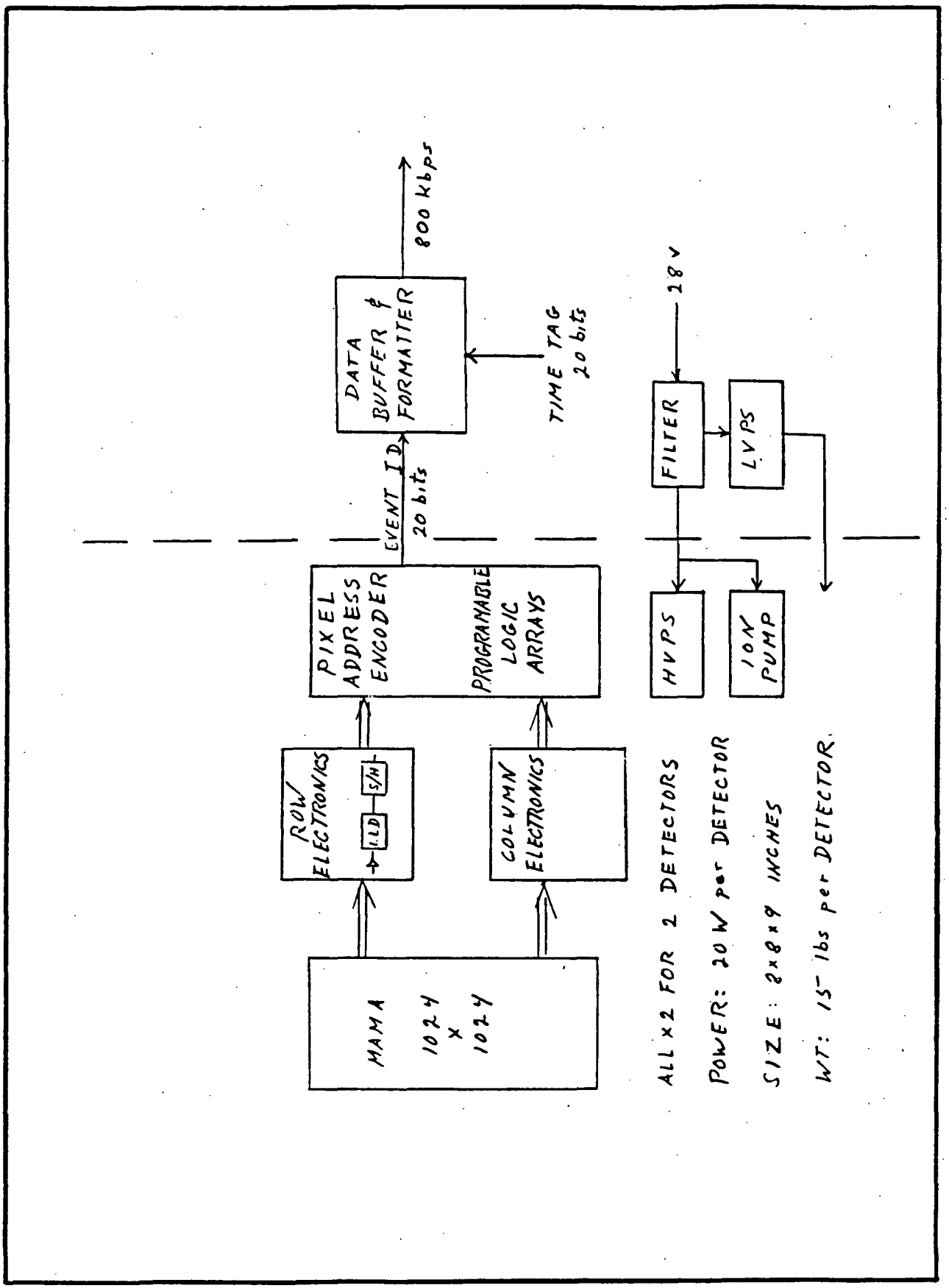

Figure 8. P/OF-UVCS Detector Electronics (replaces shaded area of Figure 7).